Preventive Oral Treatment with Resveratrol Pro-prodrugs Drastically Reduce Colon Inflammation in Rodents

Mar Larrosa[1], Joao Tomé-Carneiro[1], María J. Yáñez-Gascón[1], David Alcántara[2], María V. Selma[1], David Beltrán[1], María T. García-Conesa[1], Cristina Urbán[1], Ricardo Lucas[2], Francisco Tomás-Barberán[1], Juan C. Morales[2]*, and Juan Carlos Espín[1]*.

Research Group on Quality, Safety and Bioactivity of Plant Foods, Department of Food Science and Technology, CEBAS-CSIC, 30100 Campus de Espinardo, Murcia, Spain. Department of Bioorganic Chemistry, Instituto de Investigaciones Químicas (IIQ), CSIC-Universidad de Sevilla, 41092 Sevilla, Spain.

Running Title: Combating colon inflammation with resveratrol pro-prodrugs.

[1]CEBAS-CSIC
[2]IIQ-CSIC-Univ. Sevilla

   *To whom correspondence should be addressed: J.C.M. (Phone: +34-954-489561. Fax: +34-954-460565. E-mail: jcmorales@iiq.csic.es) or J.C.E. (Phone: +34-968-396344. Fax: +34-968-396213. E-mail: jcespin@cebas.csic.es).

Abbreviations: anh., anhydrous, AUC, area under the curve; BUT, mice group fed with *trans*-resveratrol-3-*O*-(6'-*O*-butanoyl)-β-D-glucopyranoside (**6**); *t*-BuOH, *tert*-butanol, C_{max}, maximum concentration; COX-2, cyclooxigenase-2; DAI, disease activity index; DCM, dichloromethane; DIGLUC, mice group fed with *trans*-resveratrol-3,4'-di-β-D-glucopyranoside (**4**); DMF, dimethylformamide; DSS, dextran sodium sulphate; GM-CSF, granulocyte macrophage colony-stimulating factor; HED, human equivalent dose; HRMS, high resolution mass spectrometry; HSP70, 70 kDa heat shock protein; IBDs, inflammatory bowel diseases; IGF-1, insulin growth factor type 1; IL-3, interleukin-3; IL-6, interleukin-6; IL-10, interleukin 10; MeOH, methanol; MIG, IFNγ-inducible T cell chemoattractant monokine; MIP-1γ, macrophage inflammatory protein-1-gamma (CCL9); MOP, myeloperoxidase; MS, molecular sieves, MTT, (3-(4,5-Dimethylthiazol-2-yl)-2,5-diphenyltetrazolium bromide; NF-κB, nuclear factor kappa-B; MW, molecular weight; NMR, nuclear magnetic resonance spectroscopy; OCT, mice group fed with *trans*-resveratrol-3-*O*-(6'-*O*-octanoyl)-β-D-glucopyranoside (**7**); PGE_2, prostaglandin E_2; PIC, mice group fed with *trans*-piceid (compound **2**); PON2, paraoxonase-2, PTGES, prostaglandin E synthase; RES, mice group fed with free resveratrol (3,5,4'-trihydroxy-*trans*-stilbene, compound **1**); r.t., room temperature; SIRT1, silent mating type information regulation 2 homolog 1; sTNF RI, p55 subunit of the TNFα receptor (TNFRp55, CD120a); TBDMS, *tert*-butyldimethylsilyl; THF, tetraydrofuran; TLC, thin layer chromatography; VCAM, vascular cell adhesion molecule.

Abstract

There is no pharmaceutical or definitive surgical cure for inflammatory bowel diseases (IBDs). The naturally-occurring polyphenol resveratrol exerts anti-inflammatory properties. However, its rapid metabolism diminishes its effectiveness in the colon. The design of prodrugs to targeting active molecules to the colon provides an opportunity for therapy of IBDs. Herein we explore the efficacy of different resveratrol prodrugs and pro-prodrugs to ameliorate colon inflammation in the murine dextran sulphate sodium (DSS) model. Mice fed with a very low dose (equivalent to 10 mg for a 70 kg-person) of either resveratrol-3-*O*-(6'-*O*-butanoyl)-β-D-glucopyranoside **6** or resveratrol-3-*O*-(6'-*O*-octanoyl)-β-D-glucopyranoside **7** did not develop colitis symptoms and improved 6-fold the disease activity index (DAI) compared to resveratrol. Our results indicate that these pro-prodrugs exerted a dual effect: 1) they prevented the rapid metabolism of resveratrol and delivered higher quantities of resveratrol to the colon and 2) they reduced mucosal barrier imbalance and prevented diarrhea, which consequently facilitated the action of the delivered resveratrol in the colon mucosa.

Introduction

The term 'inflammatory bowel diseases' (IBDs) groups a wide set of clinical manifestations and presentations whose main characteristic is the chronic inflammation of the gastrointestinal tract. The major IBD forms, Crohn's disease and ulcerative colitis affect millions of individuals. Although the etiology and pathogenesis of IBDs are poorly understood, the most accepted theory includes the loss of balance between host susceptibility, enteric microbiota and mucosal immunity. This results in an exacerbated immune system response with an imbalance of pro-inflammatory cytokines, adhesion molecules and reactive oxygen metabolites provoking tissue injury[1].

Treatments for IBDs are restricted to controlling symptoms, maintaining remission and preventing relapse. Acute treatment uses antibiotics and anti-inflammatory drugs, such as corticosteroids and aminosalicylates. Sulfasalazine and 5-aminosalicylates are used in the management of mild to moderate disease, whereas the glucocorticoids remain the primary therapy for patients suffering from moderate to severe disease. However, prolonged use of corticosteroids has significant side-effects preventing their use for long-term treatments[2]. At the present time, there is no pharmaceutical or definitive surgical cure for IBDs[2]. Therefore, the search for new drug treatments remains absolutely necessary.

A limitation to the use of orally administered drugs in the treatment of IBDs is that they undergo absorption from the upper parts of the gastrointestinal tract before reaching the colon. This has two major drawbacks, the absorption, conjugation and further excretion of a high proportion of the drug without reaching the colon as well as the potential non-desirable systemic effects of some drugs. In this context, the design of pro-drugs targeting active molecules to the colon provides an opportunity to improve the therapeutic potential of drugs intended for topical therapy of the intestinal mucosa[3].

Polyphenols, plant secondary metabolites abundant in our diet through the intake of fruits and vegetables, have been reported to exert a number of health-beneficial effects including the prevention and/or amelioration of cardiovascular diseases and cancer[4]. Among polyphenols, *trans*-resveratrol (**1**) (Figure 1), naturally occurring in grapes and wine, has shown anti-platelet, antioxidant, antitumor and anti-inflammatory activities[5]. Resveratrol has been reported to ameliorate the inflammation status in mice and rat IBD models[6-8]. Recently, our group demonstrated that a human equivalent dose (HED) of 10 mg resveratrol per day for a 70 kg person for 20 days was able to ameliorate colon inflammation in an IBD

rat model[7]. However, like other phenolics, resveratrol is rapidly absorbed and conjugated by Phase II enzymes to yield mostly sulphate and glucuronate derivatives[9], which reduces resveratrol delivery to the colon and decreases its topical effectiveness in the colon mucosa.

Herein we explore the efficacy of different resveratrol prodrugs and pro-prodrugs to ameliorate colon inflammation in a colitis-induced mouse model. We hypothesized that increasing the delivery of resveratrol to the colon could improve its anti-inflammatory effects in the colon mucosa. We have prepared two series of resveratrol derivatives; the first one with glucosyl modifications, inspired by the natural molecule *trans*-piceid (**2**) (Figure 1), and the second one with glucosyl- and acyl- modifications, by attaching fatty acid groups of different length to the piceid. Three candidates, *trans*-resveratrol-3,5-di-*O*-β-D-glucopyranoside (**4**), *trans*-resveratrol-3-*O*-(6'-*O*-butanoyl)-β-D-glucopyranoside (**6**) and *trans*-resveratrol-3-*O*-(6'-*O*-octanoyl)-β-D-glucopyranoside (**7**), (Figure 1) were selected for in vivo studies after preliminary in vitro cell assays. We reasoned that a preventive oral treatment with low doses of the prodrugs would protect the mucosal barrier from inflammation avoiding disease development. Mice were fed with 2.1 mg/kg day (HED of 10 mg for a 70 kg person) of each derivative for 3 weeks prior to the induction of colitis for 8 days. The protective effects observed for both **6** and **7** were very remarkable despite the very low dose assayed. Mice fed with compounds **6** or **7** hardly developed any symptoms of colitis as evidenced by various markers: disease activity index, serum haptoglobin level, colon length and tissue damage, colonic microbiota counts, myeloperoxidase activity, prostaglandin PGE_2 production, and levels of several cytokines in the colon tissue. Our results suggest that compounds **6** and **7** exerted a dual effect: 1) higher delivery of RES quantities to the colon and 2) reduction of the mucosal barrier imbalance which prevented diarrhea and, consequently, improved the action of the delivered RES in the colon mucosa.

Results

Synthesis. Glucosylated resveratrol derivatives **3-5** were prepared following the strategy reported by Zhang et al[10] with modifications (Scheme 1). Random TBDMS-protection of resveratrol **1** and subsequent chromatographic separation afforded the four possible phenolic alcohol precursors **11**, **12**, **13**, **14** and fully silylated resveratrol **15** (24, 18, 6, 22 and 7% yields, respectively). The amount of fully protected **15** was reduced from 27 to 7% just by two additions (during 15 min each) of 1+0.5 equivalents of TBDMSCl (3h interval) with respect to the previously reported 1+1 equivalents of TBDMSCl added in two shots (also 3h interval). Glycosylation was carried out using 2,3,4,6-tetra-*O*-benzoyl-D-glucopyranosyl trichloroacetimidate **16** as the glycosyl donor[11], much more common and simpler to prepare than the previously used trifluoroacetimidate derivative[10]. However, the yields of resveratrol derivatives monoglucosylated (**19**) and diglucosylated (**17** and **18**) compounds were slightly lower (60, 40 and 64%, respectively) than those reported with the trifluoroacetimidate donor. One step-deprotection with aqueous 3N NaOH in MeOH-THF afforded compounds **3**, **4** and **5** (50, 83, 84% yields, respectively).

Piceid acyl derivatives **6** to **10** were prepared in one-step by enzymatic acylation of piceid **2** using *Thermomyces lanuginosus* lipase immobilized on granulated silica (Lipozyme TL IM) (Scheme 2). The reactions were carried out in *tert*-butyl alcohol and the acylating agents were the corresponding fatty acid vinyl esters. Short column chromatography of the reaction mixtures produced pro-prodrugs **6-10** in very high yields (88-97%).

In vitro Anti-inflammatory and Cell Metabolism Assays. To test whether these structural modifications of the resveratrol molecule had any effect on the capacity of resveratrol to reduce prostaglandin E_2 (PGE_2) synthesis under inflammatory conditions, we measured the production of PGE_2 by human colon CCD18-Co cells after co-stimulation with 1 ng/mL of IL-1β and the synthesized resveratrol derivatives for 18 h (Figure S1). The inflammatory cytokine IL-1β caused a significant increase (100-fold) in the PGE_2 levels ($P < 0.01$). Co-treatment with 1 μM of resveratrol (**1**) partially prevented the production of PGE_2 which was completely eliminated by resveratrol concentrations

5

ranging between 2.5 and 25 µM. Co-treatment with 25 µM of compound **3** partially reduced PGE$_2$ production whereas compounds **2**, **4** and **5** did not prevent PGE$_2$ induction (Figure S1A).

All the acyl-glucosyl- derivatives, at concentrations in the range from 1 to 7.5 µM, showed anti-inflammatory activity by reducing PGE$_2$ production (Figure S1B). Concentrations higher than 10 µM (results not shown) of the compounds **6** to **10**, in particular of the compounds **8**, **9** and **10**, were cytotoxic to these cells (as measured by the MTT method) upon 8 h of incubation and were not further considered.

The chemical stability and metabolism of resveratrol derivatives were evaluated after incubation with human colon cancer Caco-2 cells. This cancer cell line was chosen since its metabolism is faster than that of normal cells such as CCD18-Co. Cell media samples were analyzed by LC-MS-MS. Representative chromatograms of cell media samples after incubation of Caco-2 cells with resveratrol glucosyl-derivatives for 6 h are shown in Figure S2**.** Overall, the glucosyl modifications conferred protection to **1** by retarding its metabolism since no direct Phase II conjugation (glucuronidation, sulphation, methylation, etc.) of the glucosyl-derivatives was detected. The only conjugated metabolites detected were those of the resveratrol (mostly glucuronides) which were formed after the hydrolysis of the glucosyl-derivatives and subsequent conjugation of resveratrol by Phase II enzymes. From all the glucosyl derivatives tested, compound **4** was the most resistant to hydrolysis since a high proportion of this compound remained intact in the cell medium even after 24 h of incubation (results not shown) providing a slow release and metabolism of the active molecule resveratrol. Although compound **4** did not show anti-inflammatory activity in the cell model, its resistance to be hydrolyzed and conjugated in the cell culture suggested that it might be a good candidate as a pro-prodrug to increase the delivery of resveratrol to the colon.

Regarding the cell metabolism of glucosyl-acyl-derivatives (Figure S3), all the compounds presented a similar trend. The glucosyl-acyl modification also conferred protection to resveratrol by slowing down their metabolism. Conjugated resveratrol metabolites were only detected upon hydrolysis of glucosyl-acyl-derivatives and subsequent resveratrol conjugation by Phase II enzymes. Compounds **6** and **7** were selected for the in vivo inflammatory assays due to their higher stability compared to compounds **8**, **9** and **10,** and also to their direct in vitro anti-inflammatory activity.

Mice Weight and Disease Activity Index (DAI). Mice were fed for 21 days with standard mouse chow supplemented with 2.1 mg/kg day of the different compounds. The abbreviations RES, PIC, DIGLUC, BUT and OCT refer to the mice groups whose diets were supplemented with compounds **1**, **2**, **4**, **6** or **7**, respectively. Afterwards, 1% DSS was included in the drinking water for 8 days. Mice were still fed with each of the compound for six more days in the absence of DSS (post-treatment phase) (Scheme S1A). Food and water intake as well as stool blood, stool form, and body weight were monitored daily for the whole experimental period (35 days). There were no significant differences in the food and water intake among the different groups (data not shown). The body weight increased at a similar rate in all the groups during the 21 days pre-feeding period (Figure S4). Upon DSS administration, mouse weight decreased very rapidly in the DSS, RES, PIC and DIGLUC groups, however, DSS had no effect on the weight of the animals pre-fed with compounds **6** or **7** (BUT and OCT groups, respectively), which behaved like the control group. During the recovery phase, the weight slowly increased in the affected groups, the weight recovery being faster in the DIGLUC group.

The DAI value (which combines stool blood, stool consistency and weight loss) increased in all the groups after DSS administration although much lower DAI values were clearly obtained in the last four days of DSS consumption for BUT and OCT groups (Figure 2a). During the recovery phase, both BUT and OCT groups reached DAI values close to those of the control untreated group whereas the rest of the treated groups still exhibited higher DAI values than the control animals (Figure 2a).

Mice from the DSS-treated group (animals fed with chow diet only) showed ataxia, hair brightness loss, alopecia, leanness and severe rectal bleeding (Figure S5). However, the animals fed with the resveratrol prodrugs for 3 weeks prior to DSS consumption, showed a substantial improvement in their appearance in the following order: **7** ≈ **6** >> **4** ≈ **2** ≈ **1** > DSS. The improvement was most remarkable in the case of mice fed with compounds **6** or **7** at day 29 (Figure S5) which, based on their external appearance, seemed not to be affected by DSS consumption.

In a separate set of experiments in which mice were not pre-fed with any of the compounds prior to DSS administration (Scheme S1B), no differences in the DAI index were observed among the groups (Figure S6). These results clearly indicated a preventive effect rather than a therapeutic effect of the low doses of the compounds **6** and **7** tested (2.1 mg/kg day).

7

Colon Length. Colon shortening is a well-known feature of colon inflammation in the murine DSS model. Mice in the control group had an average colon length of 8.9 ± 0.4 cm which was reduced to 6.3 ± 0.2 cm in the DSS group ($P < 0.01$) (Figure 2b). The colon length shortening caused by DSS was only significantly prevented in the groups of animals pre-fed with compounds **6** or **7**, which had colon lengths of 7.7 ± 0.5 and 8.2 ± 0.5 cm, respectively, ($P < 0.004$) (Figure 2b).

Myeloperoxidase (MPO) Activity. MPO activity is usually increased in the colon mucosa of IBD patients as a result of leukocyte infiltration. As expected, MPO activity was induced 30-fold ($P < 0.01$) in the mice colon mucosa upon DSS administration for 8 days. This increase was only significantly reduced upon pre-treatments with compounds **6** (3.7-fold) and **7** (7.2-fold) ($P < 0.01$) (Figure 2c).

Prostaglandin (PGE$_2$) Levels. PGE$_2$ is an important pro-inflammatory lipid mediator that is produced in excess in the colon mucosa of IBD patients. PGE$_2$ levels increased 15-fold ($P < 0.01$) in mouse colon mucosa after DSS treatment. Pre-feeding with **6** or **7** attenuated the induced levels of PGE$_2$ by 2.5- and 3.5-fold ($P < 0.01$), respectively (Figure 2d), whereas the rest of the compounds were not able to reduce PGE$_2$ levels after DSS administration.

Histological Evaluation. Microscopically, colon samples from control group (Figure 3a) showed the normal histology of the mouse distal colon. Damage to the colonic mucosa assessed by total histological score was significantly higher ($P < 0.005$) in the DSS group than in the other groups (Table S1). In the DSS group, colonic sections showed typical inflammatory changes in colonic architecture such as severe crypt and surface epithelial loss as well as strong infiltration of inflammatory cells (mononuclear cells, neutrophils and eosinophils) (Figure 3b). A complete disruption of the epithelial architecture was observed in some areas. In general, pre-treatment with the resveratrol prodrugs reduced the morphological signs of cell damage and preserved the mucosal architecture (Figure 3c-g). In some areas, the epithelium remained almost intact. These protective effects were most remarkable in animals pre-fed

with the compounds **6** or **7** (Figure 3f,g), particularly in the case of the OCT group, fed with **7** (Figure 3g, Table S1).

Cytokine Array of Colon Samples. Imbalance of cytokines is contributing to the pathogenesis of IBD. Cytokines levels in time and space modulate the development, recurrence and exacerbation of the inflammatory process in IBD. Forty cytokines (Figure S7) were analyzed in the colon mucosa of mice at the end of the DSS administration. Proteins exhibiting significant changes ($P < 0.05$) are shown in Figure 4 and Figure S8. DSS increased the levels of soluble TNFα receptor type I (sTNF RI, also known as TNFRp55; Figure 4a) by 2-fold ($P < 0.05$), macrophage inflammatory protein-1-gamma (MIP-1γ, also known as CCL9; Figure 4b) by 3-fold ($P < 0.05$), interferon-gamma-inducible T cell chemoattractant monokine (MIG; Figure 4c) by 2-fold ($P < 0.05$) and interleukin-6 (IL-6; Figure 4d) by 3-fold ($P < 0.05$). Pre-administration of compounds **1**, **2**, **4**, **6** and **7** decreased the expression of these cytokines induced by DSS. The compounds **6** and **7** showed a stronger inhibition of the expression of sTNF RI (Figure 4a) and MIP-1γ (Figure 4b) than the rest of the resveratrol derivatives, reaching protein levels similar to those of the control animals. The levels of MIP-1γ were also detected and measured in serum but were not affected by DSS treatment and no differences were found among the groups (results not shown). Other proteins such as the granulocyte macrophage colony-stimulating factor (GM-CSF; Figure 4e) and interleukin-10 (IL-10; Figure 4f) were not significantly affected by DSS and only compounds **6** and **7** significantly decreased the levels of these two cytokines, even below those determined for control animals. Interleukin-3 (IL-3; Figure S8) was not induced by DSS. However, all the resveratrol derivatives significantly increased the levels of this cytokine. IL-3 was not detected in serum.

Acute Phase Proteins. Both haptoglobin and fibrinogen are acute phase proteins that determine systemic inflammation and are usually elevated in IBD patients. DSS increased the levels of serum haptoglobin (Figure 5a) and fibrinogen (Figure 5b) by 9-fold and 2-fold ($P < 0.05$), respectively. Pre-feeding with **1**, and more markedly**,** with **6** or **7** reduced haptoglobin values to those of the control animals (Figure 5a). The compounds **4**, **6** and **7** also prevented the increase of fibrinogen serum level induced by DSS (Figure 5b).

9

Fecal Microbiota. An altered gut microbial composition could be involved in the pathogenesis of IBD. On the other hand, high counts of some specific microbial groups such as bifidobacteria, lactobacilli and clostridia have been correlated with an improvement of the intestinal health. Groups pre-treated with the resveratrol prodrugs showed a significant increase ($P < 0.001$) of fecal lactobacilli and bifidobacteria counts after 21 days of dietary supplementation with each of the compounds (Figure 6a,b) whereas, animals fed on un-supplemented chow had constant numbers of these bacteria. The DSS induced a marked decrease of the counts of these two groups of bacteria in the untreated group as well as in the groups pre-fed with **1**, **2** and **4** (Figure 6a,b). However, lactobacilli and bifidobacteria counts continue raising in the groups treated with **6** or **7** (Figure 6a,b).

Regarding clostridia, enterobacteria and *E. coli*, the compounds **2** and **4** were not evaluated as these experiments were focused on the most effective compounds (**6** and **7**) and using different controls including the unmodified resveratrol molecule (**1**). Clostridia counts increased slightly in the RES (compound **1**), BUT (compound **6**) and OCT (compound **7**) groups after 21 days of pre-feeding but were only statistically significant in the case of the OCT group (Figure 6c). As in the case of lactobacilli and bifidobacteria counts, DSS administration drastically reduced the levels of clostridia in the DSS group (no-pretreatment) and in the RES group (Figure 6c) but not in the BUT and OCT groups (Figure 6c).

A significant growth induction of *Escherichia coli* and enterobacteria ($P < 0.01$), was observed upon DSS administration (Figure 6d). *E. coli* induction was significantly diminished ($P < 0.01$) by pre-feeding with compounds **1**, **6** or **7**. Enterobacteria were only significantly decreased ($P < 0.01$) by **6** and **7** (Figure 6d).

Absorption, Metabolism and Gastro-Intestinal Transit Kinetics of Resveratrol Derivatives. For the metabolic studies, healthy mice (Scheme S2A) were intragastrically administered with **1**, **2**, **4**, **6**, or **7** at a much higher dose (84 mg/kg) than that used for the intestinal inflammatory assays (2.1 mg/kg). This enabled us to detect the parent compounds as well as the different resulting metabolites in the gastrointestinal tract and in plasma. Stomach, small intestine, colon and plasma samples were taken at nine time-points after DSS administration and were monitored by HPLC-MS-MS.

10

Figure S9 shows the evolution of the concentration of the initially administered parent compounds (**1**, **2**, **4**, **6** and **7**) (Figure S9A) and their hydrolysis products piceid (**2**) and free resveratrol (compound **1**) (Figure S9B and S9C, respectively) in the stomach. The corresponding AUC (area under the curve) and C_{max} (maximum concentration) values are shown in Table S2. Resveratrol (**1**) remained intact in the stomach 8 hours after intragastric administration (Figure S9A) and showed very high AUC and C_{max} values that diminished upon the intestinal transit and absorption. The rest of the dosed compounds (**2**, **4**, **6** and **7**) were partially hydrolyzed in the stomach to release different quantities of the intermediate piceid (**2**) (Figure S9B) and of the final hydrolysis product, free resveratrol (**1**) (Figure S9C). The hydrolysis process continued in the small intestine (Figure S10). Glucuronide and sulphate resveratrol derivatives were also detected in the small intestine (results not shown). Regarding the levels of circulating resveratrol metabolites (mainly resveratrol-glucuronide) in the systemic bloodstream after the ingestion of the glucosyl and acyl-glucosyl prodrugs, it was found that the AUC and C_{max} values were approximately 10-fold lower and between 3- to 30-fold lower, respectively, than those determined after ingestion of compound **1** (Figure S11 and Table S2). These results clearly indicated that all the glucosyl and acyl-glucosyl modifications diminished resveratrol absorption and conjugation. Consequently, the use of these prodrugs should increase the delivery of resveratrol to the colon, a fact that was confirmed by higher AUC and C_{max} values of free resveratrol detected in the colon (Figure 7a, Table S2). Only 4.5% of resveratrol ingested as such (**1**) reached the colon whereas the highest C_{max} values were observed for **2**, **6**, and **7**. None of the initially administered parent compounds were detected in the colon.

The differences between the results obtained with **1**, **6** and **7** were accentuated in mice with DSS-induced colitis (Scheme S2B). In this second experiment we focused only on the prodrugs with the highest delivery of resveratrol to the colon (**6** and **7**) and compared them to resveratrol itself (**1**). One time-point (4 h post-ingestion) was analyzed (Figure 7b). It should be noted that in healthy mice the amount of resveratrol delivered to the colon increased by 2.5- and 3.3-fold in the **6** and **7** dosed animals respectively, as compared to the **1** dosed group (Figure 7a). However, in mice pre-treated for 21 days with **6**, **7** or **1** and with DSS-induced colitis, the amount of resveratrol delivered to the colon increased by 12.6- and 28-fold in BUT (compound **6**) and OCT (compound **7**) groups, respectively, compared to the RES (compound **1**) group (Figure 7b).

11

Discussion

   The intestinal inflammatory model based on oral DSS administration is widely accepted and it has been reported to be relevant for the translation of data from mice to humans to identify and validate new therapies for IBDs[12]. Orally administered DSS disrupts the epithelial barrier causing acute clinical symptoms (diarrhea and bloody stools), epithelial crypt loss and subsequently inflammation. These inflammatory features are found in ulcerative colitis and Crohn's disease as the increased colonic permeability leads to an increased interaction between microbiota and immune system, one of the important factors on initiation of IBD.

   Resveratrol (**1**) exerts a plethora of different biological activities[5]. Previous studies have reported the amelioration of DSS-induced colitis in mouse and rat models using high[6,8] and low[7] resveratrol doses through the downregulation of COX-2 (cyclooxigenase-2) and PTGES (prostaglandin E synthase)[6,7] as well as the inhibition of NF-κB activation mediated by SIRT1 (silent mating type information regulation 2 homolog 1) induction[8]. Larrosa et al.[7] reported the regulation of genes implicated on different pathways such as interleukin 6 (IL-6) NetPath 18, HSP70, mitochondrial fatty acid oxidation, Wnt signaling and T-cell-receptor NetPath 11, as revealed by functional analysis of differentially expressed genes from colon mucosa samples of rats treated with DSS and 1 mg/kg day resveratrol[7]. In addition, the low dose of **1** treatment counteracted the deleterious effect of DSS treatment by regulating the expression of other important genes including IGF-1, leptin, VCAM, PON-2, adiponectin, SIRT3 and SIRT7[7]. Since **1** is rapidly absorbed, metabolized and excreted[9], which limits its potential use as a colon anti-inflammatory drug, it is of great interest to design resveratrol prodrugs to improve delivery of this molecule to the colon. Other anti-inflammatory drugs (naproxen, flurbiprofen, sulindac, 5-aminosalicylic acid, etc.) present similar problems and a prodrug approach has been quite successful to improve drug delivery to the colon. For example, azo derivatives as prodrugs of 5-aminosalicylic acid have shown potent anticolitic effect in a rat model[13]. In addition, colon targeting is very important in the case of steroidal

drugs to reduce side effects. In this context, a cyclization-activation prodrug strategy was validated in a murine DSS model to depress steroid absorption and consequently to reduce side effects[14].

Our preliminary in vitro inflammation assay revealed that resveratrol was the most effective anti-inflammatory molecule in a model with direct cell-molecule interaction (Figure S1). However, as resveratrol (**1**) is rapidly metabolized and excreted in vivo, a more efficient delivery of **1** to the colon should involve both protection from rapid **1** metabolism and further prodrug hydrolysis to deliver **1** to the colon. According to the in vitro inflammation and cell metabolism assays, the compounds **2**, **4**, **6** and **7** could potentially fulfill the above requirements.

The in vivo assay described in the present study implied the long-term administration of low doses of the test compounds mixed with the diet. This approach takes into account three important points: 1) oral administration, since it is a challenge to develop effective orally administered colon anti-inflammatory drugs[2]; 2) use of a very low dose (HED: 10 mg/day for a 70 kg-person). Although no significant acute toxicity has been reported for resveratrol, treatments with high resveratrol concentrations for long periods have not been evaluated so far; 3) since it is widely known that many dietary compounds can interfere with the absorption, metabolism and action of drugs[15], the prodrugs were administered mixed with the diet to consider the potential neutralizing effect of food matrix.

The mice fed with the resveratrol pro-prodrugs **6** and **7** hardly developed any intestinal inflammation symptoms which was evidenced by the overall appearance of mice as well as by the different parameters and molecular markers evaluated. In general, the lack of colitis symptoms in mice fed with **6** and **7** was confirmed by the scarce colon tissue damage (Figure 3f,g), which matched with low myeloperoxidase activity (Figure 2c) and low levels of leukocyte-derived cytokines (Figure 4a-e) determined in these groups. In addition, the levels of the pro-inflammatory mediator PGE_2 in the colon mucosa of these two groups were significantly lower than in the other groups (Figure 2d). PGE_2 is crucial for monocyte-derived dendritic cells to acquire potent T-helper cell stimulatory capacity and chemotactic responsiveness to lymph node-derived chemokines[16]. PGE_2 is a key mediator in intestinal inflammation and colorectal cancer[17]. The role of PGE_2 in IBDs appears to have a dual effect. Whereas a low PGE_2 synthesis seems to be related to the recovery of inflammatory-induced damage[18], high PGE_2 levels can exacerbate inflammatory processes[19]. Therefore, the low PGE_2 values detected in mice fed with **6** and **7**

(BUT and OCT groups, respectively, Figure 2d), also indicated that these groups hardly developed colitis. In addition, as part of the healing mechanisms upon intestinal inflammation, PGE_2 has been reported to induce IL-10 which is a known anti-inflammatory cytokine[20]. In agreement with this, our results showed no IL-10 induction after DSS treatment in both BUT and OCT groups (Figure 4f).

Cytokine arrays analyses revealed that the induction, under inflammatory conditions, of a number of cytokines such as MIG, IL-6 and especially, TNF-Rp55 (Figure 4a), MIP-γ (Figure 4b) and GM-CSF (Figure 4e) was prevented by **6** and **7**. TNF-Rp55 is the major soluble TNF-α receptor (sTNFR) in the lamina propria and submucosal regions of the colon. Mice lacking TNF-Rp55 and treated with DSS have been reported to show reduced mucosal damage, reduced infiltration of macrophages and neutrophils, and attenuated subsequent tumor formation[21]. The precise role of the granulocyte macrophage colony-stimulating factor (GM-CSF) in IBD remains to be elucidated. Whereas GM-CSF can be induced upon DSS administration[22] it has been also reported to elicit bone marrow-derived cells that promote efficient colonic mucosal healing[23]. The role of the murine MIP-1γ (CCL9) in experimental colitis has not been previously reported. Our study shows, for the first time, the induction of this chemokine in the DSS-induced experimental colitis model. CCL9 is secreted by the murine follicle-associated epithelium of Peyer's Patches and recruits CD11b^{+} dendritic cells which seem to be a critical mechanism to capture antigens and present them to CD4^{+} T cells[24]. Subsequently, T cells mount an adaptative immune response against potentially pathogenic organisms. Therefore, induction of CCL9 and consequent impairment of this process can contribute to an exacerbated inflammatory response. This induction was completely prevented by both **6** and **7** (Figure 4b). Although the role of sTNFR, PGE_2, GM-CSF and CCL9 in inflammatory bowel diseases is not fully understood, it is reasonable to argue, in accordance with our results, that keeping their values similar to those of the control (healthy) group resembles a normal intestinal homeostasis.

The mechanism by which **6** and **7** prevented DSS-induced colitis could not be simply explained by the observed increase in bifidobacteria, lactobacilli or clostridia since the other resveratrol prodrugs tested also caused a similar or even higher increase of bacteria counts before DSS administration (Figure 6). However, after DSS administration, the bacterial population was maintained or even increased in the case of **6** and **7**, while the bacterial counts dramatically decreased in the rest of the groups. Therefore, the

maintenance of bacterial counts in the BUT and OCT groups after DSS administration seemed to be a consequence of the normal mucosal barrier balance promoted by **6** and **7**. In this context, Larrosa et al.[7] hypothesized a potential synergistic effect of the induced colonic microbiota with resveratrol in the final anti-inflammatory effects observed. According to the present study, the resveratrol prodrugs-induced microbiota did not seem to be critical in the prevention of colon inflammation symptoms since **1**, **2** and **4** increased microbiota counts before DSS administration (Figure 6) but were not as effective as **6** and **7** in preventing the colitis.

In an attempt to prove our prodrug approach as a mean to achieve higher delivery of resveratrol to the target colon, the gastrointestinal transit kinetics of all the resveratrol prodrugs was evaluated. Despite the huge number of reports on resveratrol, our study also shows for the first time the monitoring of resveratrol transit through the gastrointestinal tract. In healthy mice, the maximum concentration of resveratrol was detected in the colon after 4 h of oral administration. The lowest concentration was detected in the case of mice fed with resveratrol itself (compound **1**) whereas the highest values of resveratrol were found in mice fed with **6** and **7**. These results indicated that the addition of butanoyl-glucose- and octanoyl-glucose- residues to the resveratrol molecule improved the delivery of this bioactive compound to the colon. We then hypothesized that resveratrol delivery might have been improved in mice previously fed with **6** and **7** since these animals did not suffer from diarrhea whereas animals fed with **1** did have diarrhea. Resveratrol delivery to the colon was also much higher in the DSS-treated mice in BUT and OCT groups compared to RES group (Figure 7b). Therefore, the prevention of diarrhea by **6** and **7** improved colonic resveratrol delivery in the BUT and OCT groups. Both, prevention of diarrhea and increased delivery of resveratrol to the colon seemed to be relevant in the prevention of inflammation symptoms in DSS-treated mice fed with **6** and **7**. This is even more relevant taking into account that the same pro-prodrug dose administered (2.1 mg/kg day) implies different quantities of initial resveratrol. This is important if resveratrol is the active core of the prodrugs. Considering the molecular weight of resveratrol (MW=228), the dose administered of **1** (unmodified resveratrol) was 2.1 mg/kg day (i.e., ratio = 1). However, depending on the structural modification, the initial quantity of resveratrol administered was different, i.e. compound **2** (MW=390), ratio prodrug:resveratrol = 0.58; compound **4** (MW=552), ratio = 0.41: compound **6** (MW=460), ratio = 0.5 and compound **7** (MW=515),

ratio = 0.44. Therefore, despite the lower amount of resveratrol initially administered, the colonic resveratrol delivery as well as the overall preventive effect against DSS-induced ulcerative colitis was higher for all the prodrugs than for free (unmodified) resveratrol (**1**).

The small differences found in colonic resveratrol delivery upon ingestion of **2**, **6** and **7** seem to indicate that other specific mechanisms are involved in the protective effects of **6** and **7** in this intestinal inflammatory model. A potential direct action of the compounds **6** and **7** before hydrolysis, might be possible in the upper gastrointestinal tract but not in the colon where only resveratrol was detected. Although DSS affects mainly colon distal parts, an increase in the small intestinal mucosal permeability is part of the early stages of the DSS-induced colitis which precedes the histological detectable changes[25]. It has been recently reported that DSS can affect the small intestine by producing changes in the mucosal homeostasis that can influence the colonic response after DSS treatment as well as the dimension of the inflammatory response to heal intestinal damage[26].

Butyric acid and octanoic acid, released upon hydrolysis of **6** and **7**, could also be involved in the preventive effect observed since these molecules are known anti-inflammatory short and medium fatty acids, respectively[27,28]. This scenario would involve a pro-double-drug mechanism, where the fatty acid chain and the resveratrol molecule would be playing a role side-by-side. However, the total amount of butyrate released daily upon hydrolysis of **6** could reach values of only 0.4 mg/kg (1.9 mg for a 70 kg person). It would be difficult to explain the remarkable protective effects observed in our study with such a small amount of butyrate when some studies in animals and humans with IBD reported discrete anti-inflammatory responses using 2,000-fold higher quantities of butyrate (HED 4 g for a 70 kg person)[29,30]. A similar reasoning could be applied to compound **7**. Despite the above, the beneficial effects of long-term low-dose oral administration of butyrate and octanoate in IBDs cannot be ruled out.

Our results suggest that **6** and **7** act as resveratrol pro-prodrugs with a dual activity, i.e., modulating the barrier mucosal homeostasis and delivering effectively anti-inflammatory resveratrol to the colon. This suggests that chronic consumption of **6** and **7** could be very important in a potential maintenance or remission stage of IBD to prevent relapse. It is important to remark that the low pro-prodrugs dose assayed effectively prevented colitis symptoms upon repeated oral administration before colitis

induction. In this context, the investigation of potential therapeutic effects at higher prodrugs concentrations is warranted.

Experimental Section

Chemistry. TLC was carried out on precoated Silica-Gel 60 plates F254, and stained by heating with Mostain (500 ml of 10% H_2SO_4, 25g of $(NH_4)_6Mo_7O_{24} \cdot 4H_2O$, 1g $Ce(SO_4)_2 \cdot 4H_2O$). Products were purified by flash chromatography with silica gel60 (200-400 mesh). NMR spectra were recorded on either a Bruker AVANCE 300 or ARX 400 MHz [300 or 400 MHz (^1H), 75 or 100 (^{13}C)] spectrometer, at room temperature for solutions in $CDCl_3$, D_2O or CD_3OD. Chemical shifts are referred to the solvent signal and are expressed in ppm. 2D NMR experiments (COSY, TOCSY, ROESY, and HMQC) were carried out when necessary to assign the corresponding signals of the new compounds. High resolution FAB (+) mass spectral analyses were obtained on a Micromass AutoSpec-Q spectrometer. Compound purities of test compounds **1-10** by reversed-phase HPLC (integration of chromatograms at λ=320 nm) were ≥95%.

General procedure for the synthesis of the piceid fatty acid esters 6-10. Preparation of derivatives **6-10** was carried out by regioselective enzymatic acylation of piceid **2** (from Sigma Aldrich) by the following general procedure: lipozyme TL IM (100-150 mg) was added to a mixture of piceid **2** (100-150 mg, 1 equiv) and the corresponding acylating agent (20 equiv) in 15-20 mL of tert-butyl alcohol. The mixture was stirred in an orbital shaker at 60 ºC for 16h. The enzyme was decanted and separated. The solvent was evaporated, and the product was purified by flash column chromatography (ethyl acetate/MeOH from 1:0 to 9:1) to yield the corresponding acylated piceid derivatives **6-10** (88-97%).

(E)-1-(3-(6'-O-Butyryl)-β-D-glucopyranosyloxy-5-hydroxyphenyl)-2-(4-hydroxyphenyl)ethene 6. The pure compound was obtained using vinyl butanoate as the acylating agent (170 mg, 97%). TLC (ethyl acetate) R_f 0.3. $[\alpha]_D^{20}$ -55.0 (c, 1 in MeOH). ^1H-NMR (MeOD, 300MHz), δ ppm: 7.39 (d, 2H, J=8.4Hz, H_{arom}); 7.03 (d, 1H, J=16.2Hz, C*H*=CH)), 6.86 (d, 1H, J=16.2Hz, CH=C*H*)), 6.79 (d, 2H, J_{ortho}=8.7Hz, H_{arom}), 6.74 (s, 1H, H_{arom}), 6.64 (s, 1H, H_{arom}), 6.43 (t, 1H, J=2.1Hz, H_{arom}), 4.92 (m, 1H, H-1), 4.45 (dd, 1H, J=2.1 and 12 Hz, H-6), 4.28-4.21 (m, 1H, H-6'), 3.73-3.67 (m, 1H, H-5), 3.53-3.47 (m,

2H, H-2, H-3), 3.37 (m, 1H, H-4), 2.30 (t, 2H, J=7.5Hz, CH$_2$), 1.59-1.52 (m, 2H, CH$_2$), 0.83 (t, 3H, J=7.2Hz, CH$_3$). ^{13}C-NMR (MeOD, 75MHz), δ ppm: 174.1 (C=O), 158.8, 158.2, 157.0, 139.9 (Cq$_{arom}$), 128.8 (CH=CH), 128.6, 127.5 (C$_{arom}$), 125.4 (CH=CH), 115.2 (C$_{arom}$); 107.0, 105.5, 102.9 (C$_{arom}$), 100.5 (C-1), 76.5 (C-3), 73.9 (C-5), 73.4 (C-2), 70.5 (C-4), 63.4 (C-6), 35.5 (CH$_2$), 17.9 (CH$_2$), 12.5 (CH$_3$). HRMS *m/z* calculated for C$_{24}$H$_{28}$NaO$_9$, [M+Na]$^+$: 483.1631, found: 483.1648.

(*E*)-1-(3-(6'-*O*-Octanoyl)-β-D-glucopyranosyloxy-5-hydroxyphenyl)-2-(4-hydroxyphenyl)ethene

7. The pure compound was obtained using vinyl octanoate as the acylating agent (181 mg, 92%). TLC (ethyl acetate) R$_f$ 0.35. [α]$_D^{20}$ -50.0 (c, 0.5 in MeOH). ^{1}H-NMR (MeOD, 300MHz), δ ppm: 7.38 (d, 2H, J$_{ortho}$= 8.7Hz, H$_{arom}$), 7.03 (d, 1H, J= 16.2Hz, C*H*=CH), 6.86 (d, 1H, J= 16.2Hz, CH=C*H*), 6.78 (d, 2H, J$_{ortho}$= 8.7Hz, H$_{arom}$), 6.74 (s, 1H, H$_{arom}$), 6.64 (s, 1H, H$_{arom}$), 6.43 (t, 1H, J= 2.1Hz, H$_{arom}$), 4.90(d, 1H, J= 7.3Hz, H-1), 4.45 (dd, 1H, J= 1.8 and 11.7 Hz, H-6), 4.28-4.21 (dd, 1H J= 7.5 and 11.7 Hz, H-6'), 3.73-3.68 (m, 1H, H-5), 3.51-3.45 (m, 2H, H-2, H-3), 3.45-3.33(m, 1H, H-4); 2.30 (t, 2H, J=7.5Hz, CH$_2$), 1.52-1.47 (m, 2H, CH$_2$), 1.25-1.16 (m, 8H, 4xCH$_2$); 0.86 (t, 3H, J=7.2Hz, CH$_3$). ^{13}C-NMR (MeOD, 75MHz), δ ppm:174.1 (C=O), 158.8, 158.2, 157.1, 139.9 (Cq$_{arom}$), 128.8 (CH=CH), 128.5, 127.8, 127.5 (C$_{arom}$), 125.4 (CH=CH), 115.1, 107.0, 105.2, (C$_{arom}$), 100.5 (C-1), 76.5 (C-3), 73.9 (C-5), 73.4 (C-2), 70.6 (C-4), 63.4 (C-6), 33.6, 31.4, 28.9, 28.6, 24.6, 22.3, 22.2 (CH$_2$), 13.0 (CH$_3$). HRMS *m/z* calculated for C$_{28}$H$_{36}$O$_9$, [M+Na]$^+$: 539.2257, found: 539.2269.

(*E*)-1-(3-(6'-*O*-Lauroyl)-β-D-glucopyranosyloxy-5-hydroxyphenyl)-2-(4-hydroxyphenyl)ethene 8. The pure compound was obtained using vinyl laurate as the acylating agent (138 mg, 94%). TLC (ethyl acetate) R$_f$ 0.36. [α]$_D^{20}$ -39.2 (c, 1.0 in MeOH). ^{1}H-NMR (MeOD, 300MHz), δ ppm: 7.38 (d, 2H, J$_{ortho}$= 8.4Hz, H$_{arom}$), 7.03 (d, 1H, J= 16.5Hz, C*H*=CH), 6.86 (d, 1H, J= 16.5Hz, CH=C*H*), 6.79 (d, 2H, J$_{ortho}$= 8.4Hz, H$_{arom}$), 6.74 (s, 1H, H$_{arom}$), 6.64 (s, 1H, H$_{arom}$), 6.42 (s, 1H, H$_{arom}$), 4.90 (s, 1H, H-1), 4.45 (m, 1H, H-6), 4.28-4.21 (dd, 1H, J= 7.5 and 11.7 Hz, H-6'), 3.74-3.69 (m, 1H, H-5), 3.51-3.47 (m, 2H, H-3, H-2), 3.38-3.32 (m, 1H, H-4), 2.30 (t, 2H, J= 7.5Hz, CH$_2$), 1.50 (m, 2H, CH$_2$), 1.30-1.16 (m, 16H, 8xCH$_2$), 0.90 (t, 3H, J=6.9Hz, CH$_3$). ^{13}C-NMR (MeOD, 75MHz), δ ppm:174.2 (C=O), 158.9, 158.2, 157.1, 139.9, 128.8 (Cq$_{arom}$), 128.6 (CH=CH), 127.5 (C$_{arom}$), 125.3 (CH=CH), 115.1 (C$_{arom}$), 107.0, 105.3, 102.9 (C$_{arom}$) 100.5 (C-1), 76.5 (C-3), 73.9 (C-5), 73.4 (C-2), 70.6 (C-4), 63.5 (C-6), 33.6, 31.7, 29.6, 29.4, 29.2, 29.1,

28.9, 28.7, 24.6, 22.3 (CH$_2$) 13.1 (CH$_3$). HRMS *m/z* calculated for C$_{32}$H$_{44}$NaO$_9$, [M+Na]$^+$: 595.2883, found: 595.2921.

(*E*)-1-(3-(6'-*O*-Hexadecanoyl)-β-D-glucopyranosyloxy-5-hydroxyphenyl)-2-(4-hydroxyphenyl)ethene 9. The pure compound was obtained using vinyl palmitate as the acylating agent (142 mg, 88%). TLC (ethyl acetate) R$_f$ 0.42. [α]$_D^{20}$ -40.2 (c, 1.0 in MeOH). ^{1}H-NMR (MeOD, 300MHz), δ ppm: 7.38 (d, 2H, J$_{ortho}$= 8.4Hz, H$_{arom}$), 7.03 (d, 1H, J= 16.2Hz, C*H*=CH), 6.86 (d, 1H, J= 16.2Hz, CH=C*H*), 6.79 (d, 2H, J$_{ortho}$= 8.7Hz, H$_{arom}$), 6.74 (s, 1H, H$_{arom}$), 6.64 (s, 1H, H$_{arom}$), 6.43 (s, 1H, H$_{arom}$), 4.90 (m, 1H, H-1), 4.45 (m, 1H, H-6), 4.28-4.21 (d, 1H, J= 7.6, 11.7Hz, H-6'), 3.73-3.68 (m, 1H, H-5), 3.53-3.47 (m, 2H, H-3, H-2), 3.44-3.32 (m, 1H, H-4), 2.30 (t, 2H, J= 7.5Hz, CH$_2$), 1.51 (m, 2H, CH$_2$), 1.29-1.17 (m, 24H, 12x CH$_2$), 0.91 (t, 3H, J= 6.9Hz, CH$_3$). ^{13}C-NMR (MeOD, 75MHz), δ ppm:174.1 (C=O), 158.8, 158.2, 157.1, 139.9, 128.8 (Cq$_{arom}$), 128.5 (*C*H=CH), 127.5 (C$_{arom}$), 125.4 (CH=*C*H), 115.1 (C$_{arom}$), 107.0, 105.3, 102.9 (C$_{arom}$), 100.5 (C-1), 76.5 (C-3), 73.9 (C-5), 73.4 (C-2), 70.6 (C-4), 63.5 (C-6), 33.6, 31.7, 29.7, 29.4, 29.2, 29.1, 28.9, 28.7, 24.6, 22.3 (CH$_2$), 13.0 (CH$_3$). HRMS *m/z* calculated for C$_{36}$H$_{52}$NaO$_9$, [M+Na]$^+$: 651.3509, found: 651.3549.

(*E*)-1-(3-(6'-*O*-Octadecanoyl)-β-D-glucopyranosyloxy-5-hydroxyphenyl)-2-(4-hydroxyphenyl)ethene 10. The pure compound was obtained using vinyl stearate as the acylating agent (155 mg, 92%). TLC (ethyl acetate) R$_f$ 0.46. [α]$_D^{20}$ -46.5 (c, 1.0 in MeOH). ^{1}H-NMR (MeOD, 300MHz), δ ppm: 7.38 (d, 2H, J$_{ortho}$= 8.7Hz, H$_{arom}$), 7.03 (d, 1H, J= 16.2Hz, C*H*=CH), 6.86 (d, 1H, J= 16.2Hz, CH=C*H*), 6.79 (d, 2H, J$_{ortho}$= 8.7Hz, H$_{arom}$); 6.74 (s, 1H, H$_{arom}$), 6.64 (s, 1H, H$_{arom}$), 6.43 (t, 1H, J= 2.1, H$_{arom}$), 4.91 (d, 1H, J= 7.5Hz, H-1), 4.45 (dd, 1H, J= 1.8 and 12 Hz, H-6), 4.28-4.21 (dd, 1H, J= 7.6, 11.7Hz, H-6'), 3.73-3.68 (m, 1H, H-5), 3.54-3.47 (m, 2H, H-3, H-2), 3.44-3.32 (m, 1H, H-4), 2.30 (t, 2H, J= 7.5Hz, CH$_2$); 1.50 (m, 2H, CH$_2$), 1.30-1.16 (m, 28H, 14xCH$_2$), 0.90 (t, 3H, J= 6.6Hz, CH$_3$). ^{13}C-NMR (MeOD, 75MHz), δ ppm:174.2 (C=O), 158.8, 158.2, 157.1, 139.9, 128.8 (Cq$_{arom}$), 128.6 (*C*H=CH), 127.5 (C$_{arom}$), 125.4 (CH=*C*H), 115.4 (C$_{arom}$), 107.0, 105.3, 102.9 (C$_{arom}$), 100.5 (C-1), 76.5 (C-3), 73.9 (C-5), 73.4 (C-2), 70.6 (C-4), 63.5 (C-6), 33.6, 31.7, 29.4, 29.3, 29.2, 29.1, 28.9, 28.7, 24.6, 22.3 (CH$_2$), 13.1 (CH$_3$). HRMS *m/z* calculated for C$_{38}$H$_{56}$O$_9$Na [M+Na]$^+$: 679.3822, found: 679.3857.

Animals and Experimental Design. C57BL/6J mice weighing 23 ± 2 g were provided by the Animal

Centre of the University of Murcia (Spain). All experiments were in accordance with the

recommendations of the European Union regarding animal experimentation (Directive of the European

Council 86/609/EC) and approved by and performed according to the guidelines of the Animal Ethics

Committee of the University of Murcia.

Four types of assays were carried out (see more details in Schemes S1, S2). '*Inflammation assay-1*' (7

groups with n=10 mice per group). In this study animals were fed with standard chow supplemented with

each of the following compounds: *trans*-resveratrol (**1**, RES group), *trans*-piceid (**2**, PIC group), *trans*-

resveratrol-3,5-di-*O*-β-D-glucopyranoside (**4**, DIGLUC group), *trans*-resveratrol-3-*O*-(6'-*O*-butanoyl)-β-

D-glucopyranoside (**6**, BUT group) and *trans*-resveratrol-3-*O*-(6'-*O*-butanoyl)-β-D-glucopyranoside (**7**,

OCT group) for 29 days. Colitis was induced for the last 8 days by giving 1% DSS in sterilized drinking

tap water *ad libitum*. '*Inflammation assay-2*' (7 groups, n=14 mice per group): each of the compounds

was co-administered with the DSS for 8 days (no pre-treatment). In both assays, the animal dose assayed

for each compound was 2.1 mg/kg day, which was equivalent to 10 mg of compound for a 70 kg-person

according to the human equivalent dose formula (HED[31]). Animals were randomly assigned to seven

groups, i.e., five groups with each of the compounds (**1**, **2**, **4**, **6**, or **7** plus DSS), DSS group (only DSS,

no compound) and control group (only standard diet, no compound, no DSS).

The third type of experiment was designed to investigate the bioavailability and metabolism of the

different compounds in healthy mice (*metabolism assay-1*). In this case, 84 mg of each compound/kg

was administered to the animals with an intragastric probe using ethanol:water (5:95, v:v) as vehicle.

Mice were distributed in the same groups described above with n=24 animals per group. Three mice

from each group were sacrificed at each time-point after ingestion of the compounds (0.25, 0.5, 1, 2, 4, 8,

12 and 24 h) and plasma as well as the contents of stomach, small intestine and colon were analyzed by

HPLC-MS-MS to determine the presence and concentration of parent compounds or derived metabolites.

The fourth and last experiment (*metabolism assay-2*) was focused on the detection of resveratrol in the

colon of mice subjected to the treatment described for the *inflammation assay-1* (Scheme S1A). After

pre-feeding (2.1 mg/kg day) for three weeks with the compounds **1**, **6** or **7** and colitis induction with DSS

for 8 days, animals were then given a high dose (84 mg/kg) of the compounds **1**, **6** or **7** with an

intragastric probe (n=4 animals per group). Mice were sacrificed 4 h post-ingestion of the compounds and their colon content analyzed by HPLC-MS-MS. Details for sampling procedure can be found in the Supporting Information.

Disease Activity Index. A combinatorial index of disease, or disease activity index (DAI), defined as stool blood, stool form, and weight loss[32] (see supporting information) was used to analyze the therapeutic benefit of the compounds **4**, **6** and **7** as compared to the standards **1** and **2**.

Sampling Procedure. Cell media were processed as described by González-Sarrías et al.[33]. Blood, stomach, small intestine and colon samples were processed as described by Espín et al.[34] (see supporting information)

Haptoglobin and Fibrinogen. Serum concentrations of haptoglobin and fibrinogen were determined spectrophotometrically (see supporting information).

Histological Analyses. Tissue samples from the distal colon were processed as reported elsewhere[35] and evaluated under a light microscope (see supporting information). The mucosal damage scoring system of Araki et al.[36] was used to evaluate the degree of colitis. The samples were graded 0-4 for surface epithelial loss, crypt destruction and inflammatory cell infiltration into the mucosa (maximum score = 12).

Fecal Microbiota Analysis. Microbial counts were determined in fecal samples according to Larrosa et al.[7]. Total bifidobacteria, lactobacilli, clostridia, enterobacteria and *E. coli* were determined in samples from the control group and DSS-treated group as well as in the groups pre-treated with **1**, **6** or **7**. In the groups pre-treated with **2** and **4** only bifidobacteria and lactobacilli were determined. Microbial counts were determined on days 0, 21 (before DSS administration) and 29 (after DSS administration) of the experimental period described for *inflammation assay-1* (Scheme S1).

Prostaglandin Assay. PGE_2 levels were measured in distal colon mucosa homogenates using an EIA immunoenzymatic method (Cayman Chemicals, San Diego, CA,) according to Larrosa et al.[35] (see supporting information).

HPLC Analyses. Test compounds **1-10,** cell media, plasma, stomach, small intestine and colon content samples were all analyzed by HPLC (Agilent Technologies, Waldbronn, Germany), equipped with a photodiode array detector and an HTC Ultra ESI ion-trap mass detector in series (Bruker Daltonics, Bremen, Germany). Chromatographic separations of compound-enriched diet, cell media, blood, stomach, small intestine and colon content samples as well as the identification and quantification of resveratrol metabolites were carried out as reported by Larrosa et al.[7] (see supporting information).

Antibody Arrays. Mucosa samples (40 mg) from distal colon were homogenized in PBS containing proteases inhibitors (Roche, Manhein, Germany). The mixtures were centrifuged at 15,000g for 30 min at 4 ºC. Protein concentration was measured in the supernatant using the Bradford's reagent. Colon mucosa supernatants recovered from all the animals in each group were pooled together to obtain 300 μg of protein and used to measure the levels of the 40 cytokines represented in the RayBio Mouse Inflammation Antibody Array 1 (RayBiotech, Inc., Norcross, GA, USA) according to the manufacturer's protocol. Measurements were carried out in duplicate. The cytokine presence was detected by chemiluminescence using the Chemidoc XRS equipment (Biorad Laboratories, Barcelona, Spain). Arrays were scanned with a densitometer and converted to densitometric units using the software ScanAlyze[37].

Statistical Analysis. Differences for each parameter or marker were evaluated using the ANOVA test followed by the Tukey post-hoc test. Mean values ± SD are shown. In the case of histological scores, data are represented as mean ± SEM. Statistical significance between differences in scores was calculated using the Kruskal-Wallis test and, when significant, the Mann-Witney's U-test to test for differences between two subscores. Statistic tests were carried out using the SPSS 15.0 software (SPSS Inc. Chicago, IL).

Supporting Information Available: In vitro anti-inflammatory and cell metabolism assays (Figures S1-S3); experimental design of inflammation and metabolism assays (Schemes S1, S2); evolution of mice weight (Figure S4); representative pictures of C57Bl/6 mice after DSS treatment in the absence or presence of the compounds **1**, **6** or **7** (Figure S5); evolution of DAI values upon co-administration of DSS and each of the compounds tested for 8 days without pre-treatment with the compounds for 21 days (Figure S6); histological scores for evaluating colonic tissue damage (Table S1); mouse inflammation antibody array (Figure S7); IL-3 levels colon mucosa (Figure S8); absorption, metabolism and gastro-intestinal transit kinetics of resveratrol derivatives in mice (Figures S9-11) and AUC and C_{max} values (Table S2). Supplementary Methods: In vitro anti-inflammatory activity, cell uptake and metabolism, cell viability, animals and experimental design, disease activity index and animal appearance, sampling procedure, haptoglobin and fibrinogen, prostaglandin assay, histological analysis of colon samples, fecal microbiota analysis and HPLC-MS-MS analysis. ^{1}H and ^{13}C NMR spectra of compounds **6-10**. This material is available free of charge via the Internet at http://pubs.acs.org.

References

(1)   Torres, M. I.; Rios, A. Current view of the immunopathogenesis in inflammatory bowel disease and its implications for therapy. *World J. Gastroenterol.***2008**, *14*, 1972-1980.

(2)   Engel, M. A.; Neurath, M. F. New pathophysiological insights and modern treatment of IBD. *J. Gastroenterol.* **2010,** doi: 10.1007/s00535-010-0219-3.

(3)   Patel, M., Shah, T.; Amin, A. Therapeutic opportunities in colon-specific drug-delivery systems. *Crit. Rev. Ther. Drug Carrier Sys.* **2007**, *24*, 147-202.

(4)   Williamson, G.; Manach, C. Bioavailability and bioefficacy of polyphenols in humans. II. Review of 93 intervention studies. *Am. J. Clin. Nutr.* **2005**, *81*, 243S-255S.

(5)   Baur, J. A.; Sinclair, D. A. Therapeutic potential or resveratrol: the in vivo evidence. *Nature Rev.* **2006**, *5*, 493-506.

(6)   Martín, A. R.; Villegas, I.; Sánchez-Hidalgo, M.; de la Lastra, C. A. The effects of resveratrol, a phytoalexin derived from red wines, on chronic inflammation induced in an experimentally induced colitis model. *Br. J. Pharmacol.* **2006**, *147*, 873-885.

(7)   Larrosa, M.; Yáñez-Gascón, M. J.; González-Sarrías, A.; Selma, V.; Toti, S.; Cerón, J. J.; Tomás-Barberán, F. A.; Dolara, P.; Espín, J. C. Effect of a low dose of dietary resveratrol on colonic microbiota, gene expression, inflammation markers and tissue damage in a DSS-induced colitis rat model. *J. Agric. Food Chem.* **2009**, *57*, 2211-2220.

(8)   Singh, U. P.; Singh, N. P.; Singh, B.; Hofseth, L. J.; Price, R. L.; Nagarkatti, M.; Nagarkatti, P. S. Resveratrol (*trans*-3, 5, 4'-trihydroxystilbene) induces SIRT1 and down-regulates NF-kB activation to abrogate DSS-induced colitis. *J. Pharmacol. Exp. Ther.* **2009**, *332*, 829-39.

(9)   Cottart, C. H.; Nivet-Antoine, V.; Laguillier-Morizot, C.; Beaudeux, J. L. Resveratrol bioavailability and toxicity in humans. *Mol. Nutr. Food Res.* **2010**, *54*, 7-16.

(10)   Zhang, Z., Yu, B.; Schmidt, R. R. Synthesis of mono- and di-O-β-glucopyranoside conjugates of (E)-resveratrol. *Synthesis* **2006**, *8*, 1301-1306.

(11)   Schmidt, R. R.; Michel, J.; Roos, M. Glycosylimidate, 12 Direkte Synthese von O- und O-Glycosyl-imidaten. *Liebigs Ann. Chem.,* **1984,** 1343-1357.

(12) Melgar, S.; Karlsson, L.; Rehnström, E.; Karlsson, A.; Utkovic, H.; Jansson, L.; Michaëlsson, E. Validation of murine dextran sulfate sodium-induced colitis using four therapeutic agents for human inflammatory bowel disease. *Int. Immunopharmacol.* **2008**, *8*, 836-844.

(13) Carceller, E.; Salas, J.; Merlos, M.; Giral, M.; Ferrando, R.; Escamilla, I.; Ramis, J.; García-Rafanell, J.; Forn, J. Novel derivatives as prodrugs of 5-aminosalicylic acid and amino derivatives with potent platelet activating factor antagonist activity. *J. Med. Chem.* **2001**, *44*, 3001-3013.

(14) Márquez-Ruiz, J. F.; Radics, G.; Windle, H.; Serra, H. O.; Simplicio, A. L.; Kedziora, K.; Fallon, P. G.; Kelleher, D. P.; Gilmer, J. F. Design, synthesis, and pharmacological effects of a cyclization-activated steroid prodrug for colon targeting in inflammatory bowel disease. *J. Med. Chem.* **2009**, *52*, 3205-3211.

(15) Krämer, S. D.; Testa, B. The biochemistry of drug metabolism—an introduction: part 7. Intraindividual factors affecting drug metabolism. *Chem. Biodivers.* **2009**, *6*, 1477-1660.

(16) Scandella, E.; Men, Y.; Gillessen, S.; Förster, R.; Groettrup, M. Prostaglandin E_2 is a key factor for CCR7 surface expression and migration of monocyte-derived dendritic cells. *Blood* **2002**, *100*, 1354-1361.

(17) Wang, D.; Dubois, R. N. The role of COX-2 in intestinal inflammation and colorectal cancer. *Oncogene* **2010**, *29*, 781-788.

(18) Sheibanie, A. F.; Yen, J. H.; Khayrullina, T.; Emig, F.; Zhang, M.; Tuma, R.; Ganea, D. The proinflammatory effect of prostaglandin E2 in experimental inflammatory bowel disease is mediated through the IL-23 → IL-27 axis. *J. Immunol.* **2007**, *178*, 8138-8147.

(19) Jiang, G. L.; Nieves, A.; Im, W. B.; Old, D. W.; Dinh, D. T.; Wheeler L. The prevention of colitis by E Prostanoid receptor 4 agonist through the enhancement of epithelium survival and regeneration. *J. Pharmacol. Exp. Ther.* **2007**, *320*, 883-893.

(20) Rigas, B.; Goldman, I. S.; Levine, L. Altered eicosaind levels in human colon cancer. *J. Lab. Clin. Med.* **1993**, *122*, 518-523.

(21) Popivanova, B. K.; Kitamura, K.; Wu, Y.; Kondo, T.; Kagaya, T.; Kaneko, S.; Oshima, M.; Fujii, C.; Mukaida, N. Blocking TNF-α in mice reduces colorectal carcinogenesis associated with chronic colitis. *J. Clin. Inv.* **2008**, *118*, 560-570.

(22) Xu, Y.; Hunt, N. H.; Bao, S. The role of granulocyte macrophage colony-stimulating factor in acute intestinal inflammation. *Cell Res.* **2008**, *18*, 1220-1229.

(23) Bernasconi, E.; Favre, L.; Maillard, M. H.; Bachmann, D.; Pythoud, C.; Bouzourene, H.; Croze, E.; Velichko, S.; Parkinson, J.; Michetti, P.; Velin, D. Granulocyte-macrophage colony-stimulating factor elicits bone marrow-derived cells that promote efficient colonic mucosal healing. *Inflamm. Bowel Dis.* **2009**, *16*, 428-441.

(24) Zhao, X.; Sato, A.; Dela Cruz, C. S.; Linehan, M.; Luegering, A.; Kucharzik, T.; Shirakawa, A. K.; Marquez, G.; Farber, J. M.; Williams, I.; Iwasaki, A. CCL9 is secreted by the follicle-associated epithelium and recruits dome region Peyer's patch CD11b$^+$ dendritic cells. *J. Immunol.* **2003**, *171*, 2797-2803.

(25) Venkatraman, A.; Ramakrishna, B. S.; Pulimood, A. B.; Murthy, S. Increased permeability in dextrane sulphate colitis in rats: time course of development and effect of butyrate. *Scand. J. Gastroenterol.* **2000**, *35*, 1053-1059.

(26) Kiela, P. R.; Laubitz, D.; Larmonier, C. B.; Midura-Kiela, M. T.; Lipko, M. A.; Janikashvili, N.; Bai, A.; Thurston, R.; Ghishan, F. K. Changes in mucosal homeostasis predispose NHE3 knockout mice to increased susceptibility to DSS-induced epithelial injury. *Gastroenterology* **2009**, *137*, 965-975.

(27) Tedelind, S.; Westberg, F.; Kjerrulf, M.; Vidal, A. Anti-inflammatory properties of the short-chain fatty acids acetate and propionate: A study with relevance to inflammatory bowel disease. *World. J. Gastroenterol.* **2007**, *13*, 2826-2832.

(28) Hoshimoto, A.; Suzuki, Y.; Katsuno, T.; Nakajima, H.; Saito. Y. Caprylic acid and medium-chain triglycerides inhibit IL-8 gene transcription in Caco-2 cells: comparison with the potent histone deacetylase inhibitor trichostatin A. *Brit. J. Pharmacol.* **2002**, *136*, 280-286.

(29) Di Sabatino, A.; Morera, R.; Ciccocioppo, R.; Cazzola, P.; Gotti, S.; Tinozzi, F. P.; Tinozzi, S.; Corazza, G. R.Oral butyrate for mildly to moderately active Crohn's disease. *Aliment. Pharmacol. Ther.* **2005**, *22*, 789-794.

(30) Zhang, H. Q.; Ding, T. T.; Zhao, J. S.; Yang, X.; Zhang, H. X.; Zhang, J. J.; Cui, Y. L. Therapeutic effects of *Clostridium butyricum* on experimental colitis induced by oxazolone in rats. *World J. Gastroenterol.* **2009**, *21*, 1821-1828.

(31) Reagan-Shaw, S.; Nihal, M.; Ahmad, N. Dose translation from animal to human studies revisited. *FASEB J.* **2008**, *22*, 659-661.

(32) Dieleman, L. A.; Peña, A. S.; Meuwissen, S. G.; van Rees, E. P. Role of animal models for the pathogenesis and treatment of inflammatory bowel disease. *Scand. J. Gastroenterol.* **1997**, *Suppl. 223*, 99-104.

(33) González-Sarrías, A.; Espín, J. C.; Tomás-Barberán, F. A.; García-Conesa, M. T. Gene Expression, Cell Cycle Arrest and MAPK Signalling Regulation in Caco-2 cells Exposed to Ellagic Acid and its Metabolites, Urolithins. *Mol. Nutr. Food Res.* **2009**, *53*, 686–698.

(34) Espín, J. C.; González-Barrio, B.; Cerdá, B.; López-Bote, C.; Rey, A. I.; Tomás-Barberán, F. A. The Iberian pig as a model to clarify obscure points in the bioavailability and metabolism of ellagitannins in humans. *J. Agric. Food Chem.* **2007**, *55*, 10476–85.

(35) Larrosa, M.; González-Sarrías, A.; Yañéz-Gascón, M. J.; Selma, M. V.; Azorín-Ortuño, M.; Toti, S.; Tomás-Barberán, F. A.; Dolara, P.; Espín, J.C. Anti-inflammatory properties of a pomegranate extract and its metabolite urolithin-A in a colitis rat model and the effect of colon inflammation on the phenolic metabolism. *J. Nutr. Biochem.* **2010**, doi: 10.1016/j.jnutbio.2009.04.012.

(36) Araki, Y.; Andoh, A.; Fujiyama, Y.; Bamba, T. Development of dextran sulphate sodium-induced experimental colitis is suppressed in genetically mast cell-deficient Ws/Ws rats. *Clin. Exp. Immunol.* **2000**, *119*, 264–269.

(37) Eisen, M. B.; Brown, P. O. DNA arrays for analyses of gene expression. *Methods Enzymol.* **1999**, *303*, 179-205.

Figure Legends

Figure 1. Resveratrol (**1**), piceid (**2**), and the different resveratrol pro-drugs (**3-10**) synthesized and assayed in the present study.

Scheme 1. Synthetic route to resveratrol prodrugs **3-5**[a].
[a]Conditions: (a) TBDMSCl, imidazole, anh. DMF, r. t.; (b) TMSOTf, DCM, 4Å MS; (c) 3N NaOH, MeOH-THF (5:1), 0 ºC to r.t.

Scheme 2. Synthesis of piceid fatty acid esters **6-10**[a].
[a]Conditions: (a) lipozyme® TL IM, *t*-BuOH, 60 ºC

Figure 2. (**a**) DAI values, (**b**) colon length, (**c**) myeloperoxidase activity (MPO) and (**d**) prostaglandin E_2 (PGE_2) levels in mice. Determinations of (**c**) and (**d**) were carried out in colon mucosa samples. Results shown in (**b**), (**c**) and (**d**) were determined in samples taken after 1% DSS consumption for 8 days. RES group, fed with **1**; PIC group, fed with **2**; DIGLUC group, fed with **4**; BUT group, fed with **6**; OCT group, fed with **7**. Different letters inside each graph indicates significant differences ($P < 0.05$). a, different from control; b, different from DSS; a,b, different from both control and DSS; c, different from other treatments (comparison within test compounds).

Figure 3. Histology of mouse colonic samples stained with hematoxylin and eosin. (**a**) Control group showing a normal histological section of mouse colon. (**b**) Mucosal injury induced by DSS administration for 8 days with loss of crypts and epithelial integrity as well as severe inflammatory cell infiltration. (**c, d, e, f, g**) Colonic samples from mice pre-treated for 21 days with compounds **1**, **2**, **4**, **6** or **7** (2.1 mg/kg day) before DSS administration. Prodrugs administration protected the colonic structure, especially in the case of the BUT (**f**) and OCT (**g**) groups. Epithelium, crypts and cell infiltration are indicated by arrow, square and circle, respectively. The scale bar in the first microphotograph represents 50 μm and applies to all images. Statistical analysis of significant differences is included in Table S1.

Figure 4. Effect of pre-treatment with compounds **1, 2, 4, 6** and **7** after consumption of 1% DSS on different cytokines levels in colon samples. (**a**) sTNF RI, p55 subunit of the TNFα receptor (TNFRp55, CD120a); (**b**) MIP-1γ, macrophage inflammatory protein-1-gamma (CCL9); (**c**) MIG, IFNγ-inducible T cell chemoattractant monokine; (**d**) IL-6, interleukin-6; (**e**) GM-CSF, granulocyte macrophage colony-stimulating factor and (**f**) IL-10, interleukin-10. Different letters inside each graph indicates significant differences ($P < 0.05$). a, different from control; b, different from DSS; a,b, different from both control and DSS; c, different from other treatments (comparison within test compounds).

Figure 5. Serum levels of acute phase proteins after DSS treatment. (**a**) Haptoglobin and (**b**) fibrinongen. Different letters inside each graph indicates significant differences ($P < 0.05$). a, different from control; b, different from DSS; a,b, different from both control and DSS.

Figure 6. Microbial counts in mouse feces before and after DSS treatment. (**a**) Lactobacilli: before DSS, the prodrug group was different from control and, after DSS, only **6** and **7** showed differences from DSS. (**b**) Bifidobacteria: before DSS, the prodrug group was different from control and, after DSS, only OCT and BUT showed differences from DSS. (**c**) Clostridia: before DSS, the OCT was different from control and, after DSS, OCT and BUT showed differences from DSS. (**d**) *E. coli* and enterobacteria: different letters inside graph indicates significant differences. a, different from control; b, different from DSS. Significance level ($P < 0.05$).

Figure 7. Kinetics of resveratrol delivered in the colon upon administration of resveratrol (**1**), piceid (**2**) and the resveratrol pro-prodrugs **4**, **6** and **7**. (**a**) Healthy mice (no DSS and no prodrugs pre-treatment) and (**b**) animals pre-treated with 2.1 mg/kg of compounds **1**, **6** or **7** for 3 weeks followed by DSS-induced colitis.
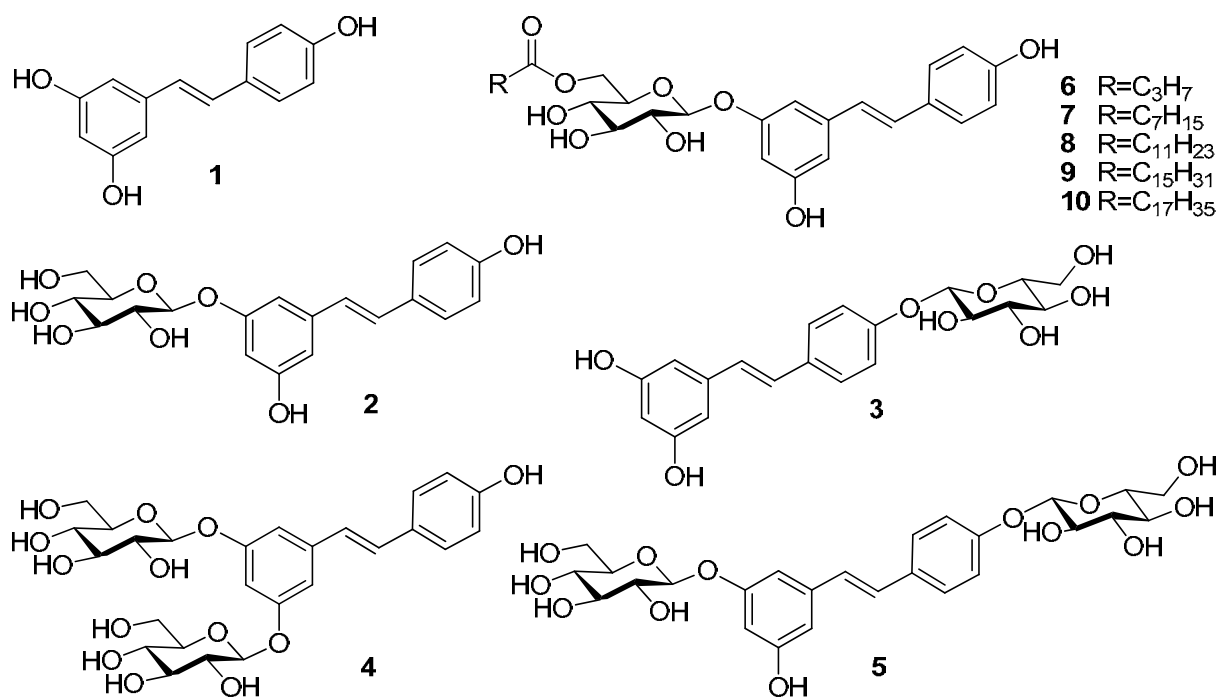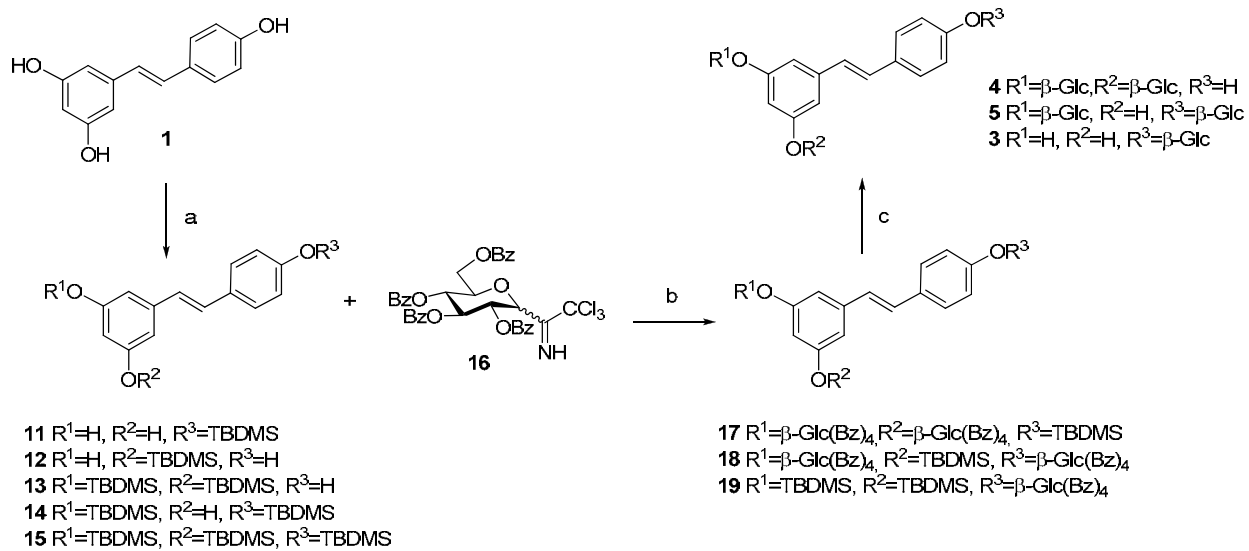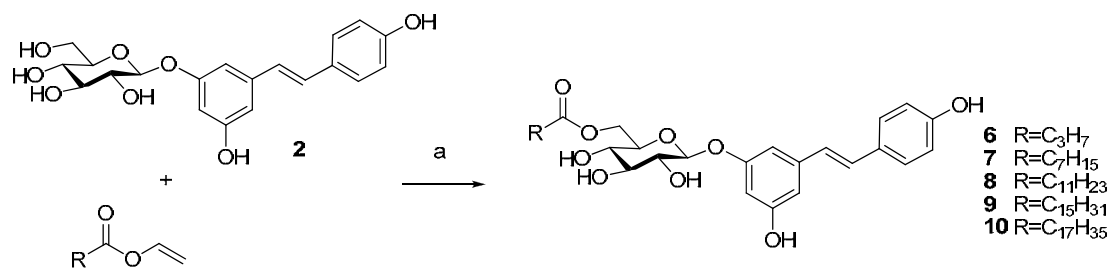
Figure 1

1

a

11 R^1=H, R^2=H, R^3=TBDMS
12 R^1=H, R^2=TBDMS, R^3=H
13 R^1=TBDMS, R^2=TBDMS, R^3=H
14 R^1=TBDMS, R^2=H, R^3=TBDMS
15 R^1=TBDMS, R^2=TBDMS, R^3=TBDMS

16

b

17 R^1=β-Glc(Bz)$_4$, R^2=β-Glc(Bz)$_4$, R^3=TBDMS
18 R^1=β-Glc(Bz)$_4$, R^2=TBDMS, R^3=β-Glc(Bz)$_4$
19 R^1=TBDMS, R^2=TBDMS, R^3=β-Glc(Bz)$_4$

c

4 R^1=β-Glc, R^2=β-Glc, R^3=H
5 R^1=β-Glc, R^2=H, R^3=β-Glc
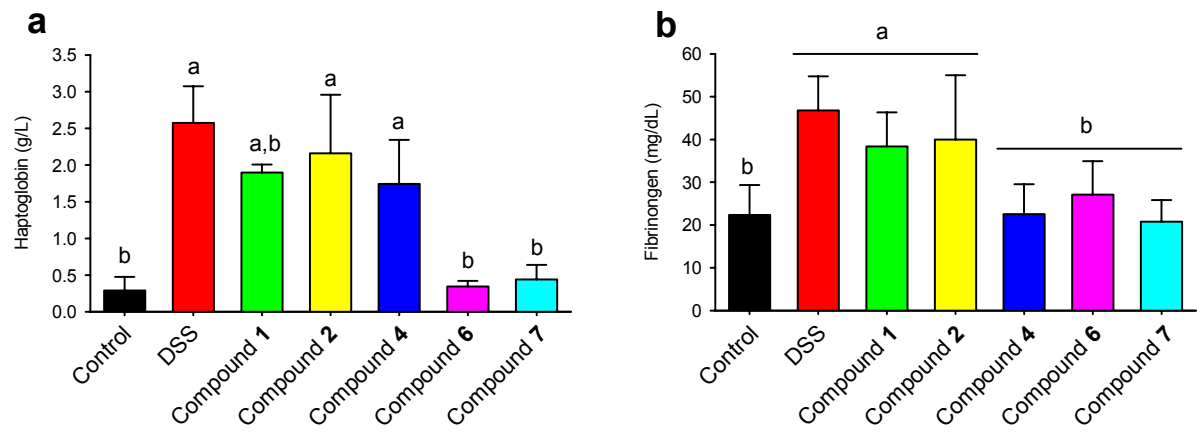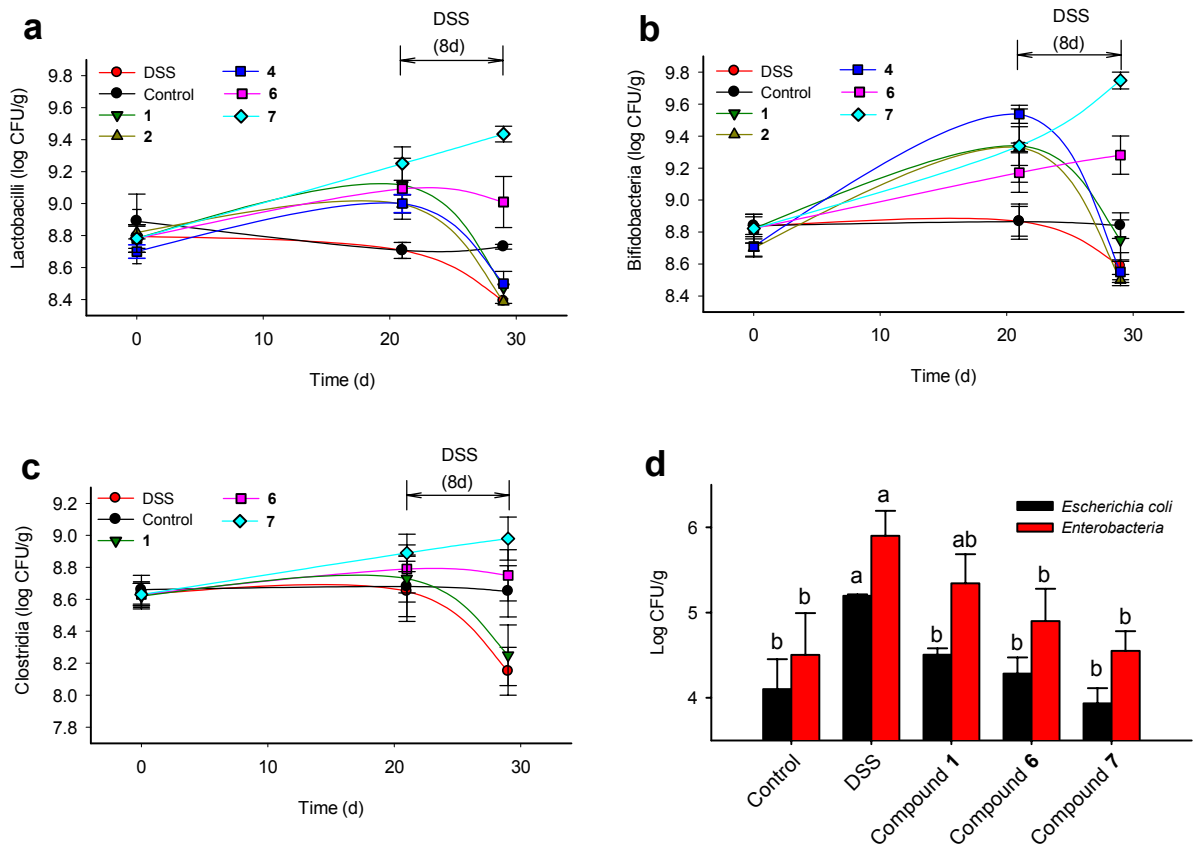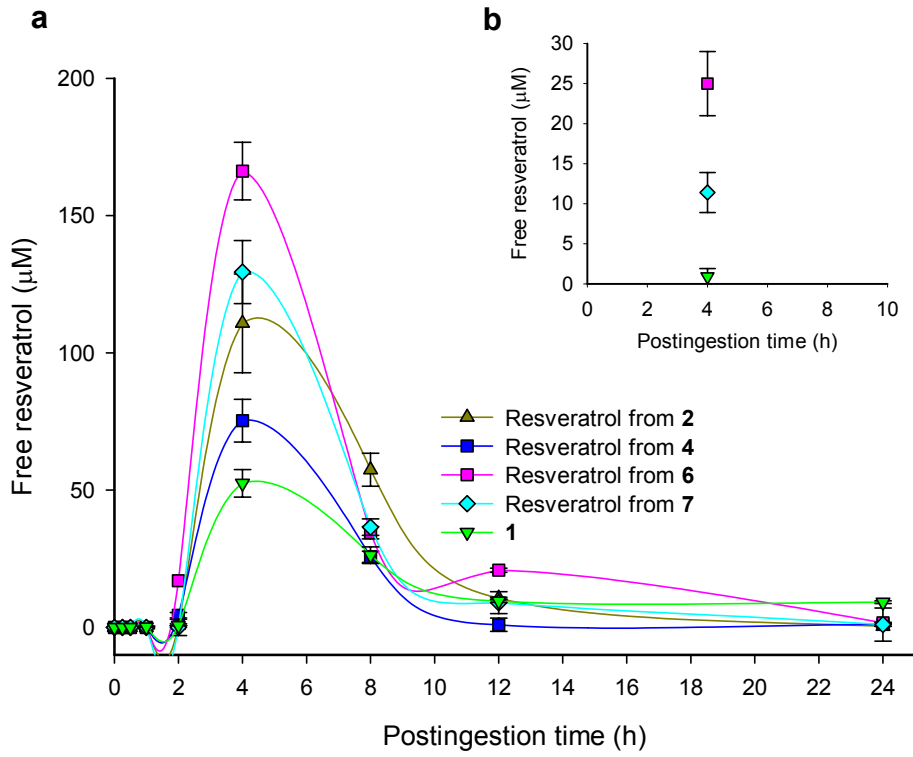**3** R^1=H, R^2=H, R^3=β-Glc

Scheme 1

Scheme 2
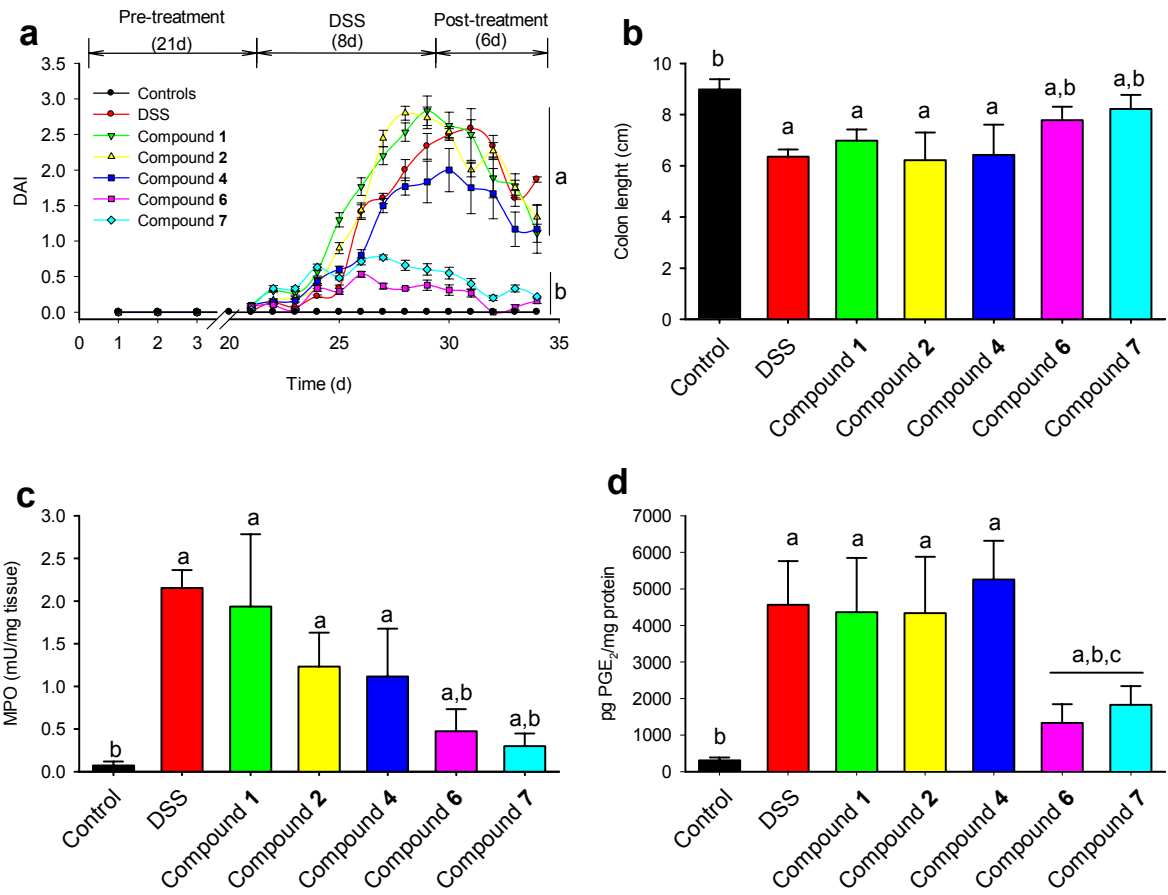
Figure 2.
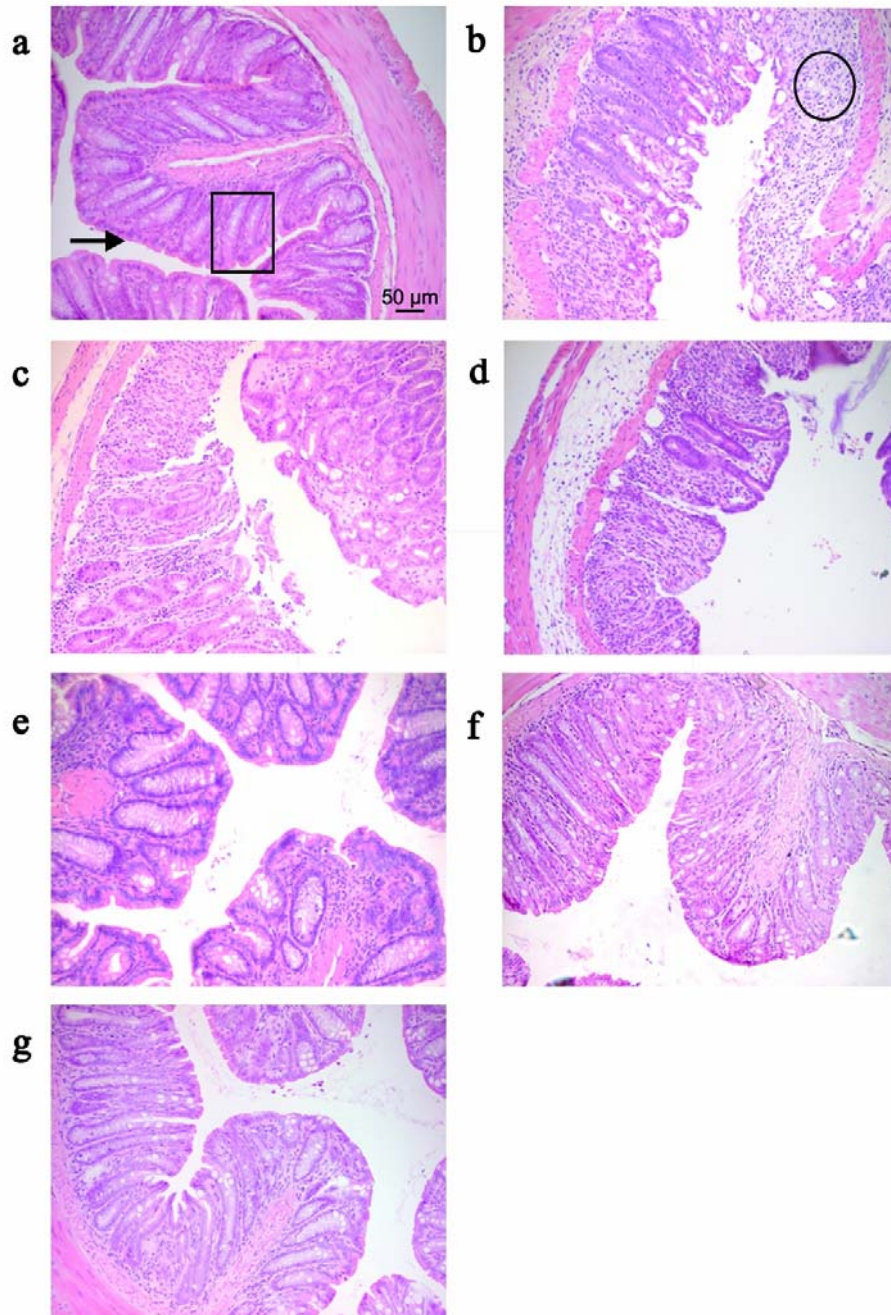
Figure 3.
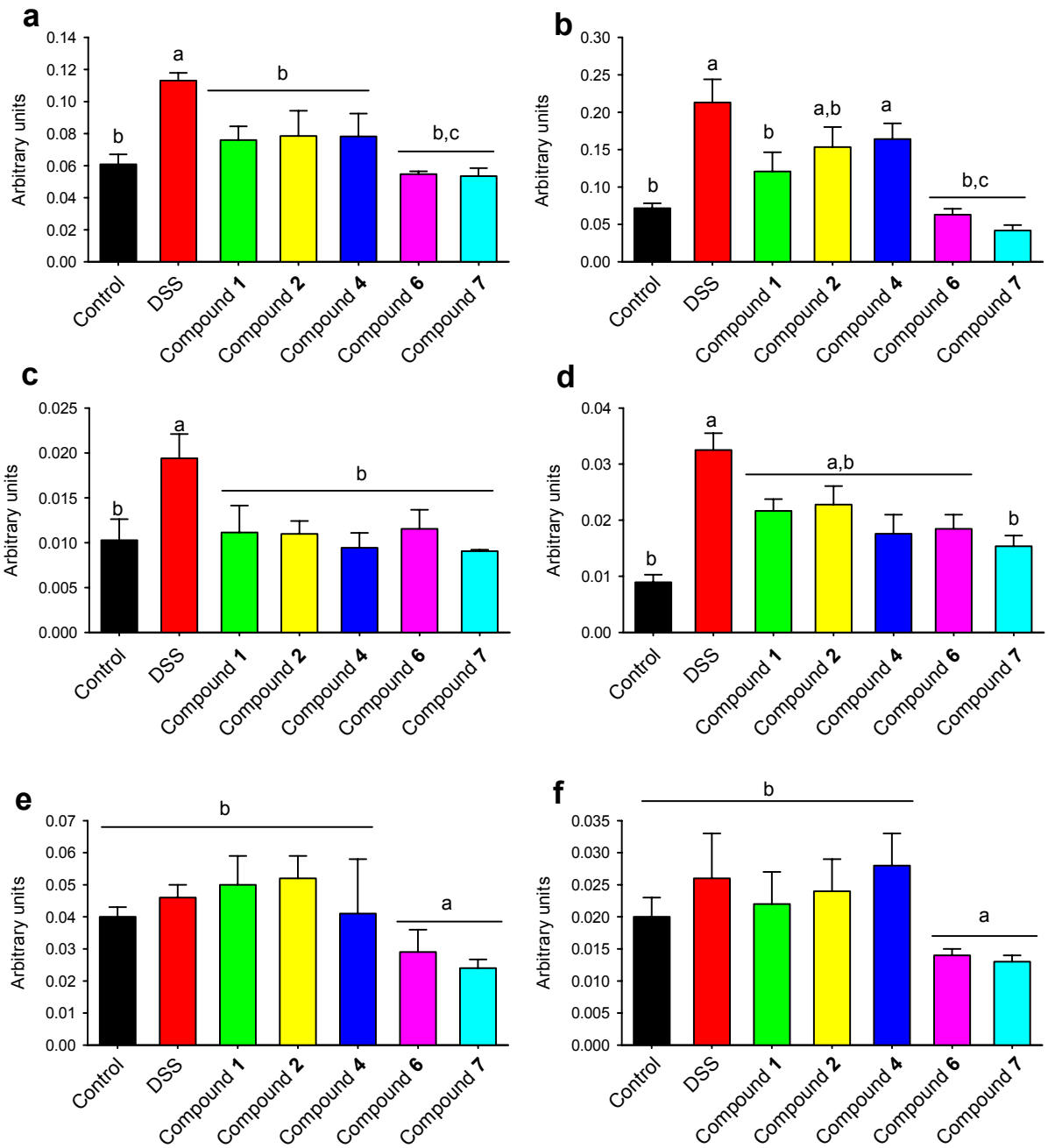
Figure 4

Figure 5

Figure 6

Figure 7

Table of Contents Graphic